Epilepsy Research (2014) **108**, 125—138

journal homepage: www.elsevier.com/locate/epilepsyres

Diffusion tensor tractography reveals disrupted structural connectivity in childhood absence epilepsy

Kaiqing Xue[a,1], Cheng Luo[a,1], Dan Zhang[a], Tianhua Yang[b], Jianfu Li[a], Diankun Gong[a], Long Chen[a], Yasser Iturria Medina[c], Jean Gotman[d], Dong Zhou[b], Dezhong Yao[a,*]

[a] *Key Laboratory for NeuroInformation of Ministry of Education, School of Life Science and Technology, University of Electronic Science and Technology of China, Chengdu, China*
[b] *Department of Neurology, West China Hospital of Sichuan University, Chengdu, China*
[c] *Neuroimaging Department, Cuban Neuroscience Center, La Habana, Cuba*
[d] *Montreal Neurological Institute, McGill University, Montreal, Quebec, Canada*

Received 23 December 2012 ; received in revised form 1 September 2013; accepted 13 October 2013
Available online 21 October 2013

KEYWORDS
Absence epilepsy;
Diffusion tensor tractography;
Structural connectivity;
Graph theory

Summary
Purpose: The structural connection patterns of the human brain are the underlying bases for functional connectivity. Although abnormal functional connectivity has been uncovered in childhood absence epilepsy (CAE) in previous electroencephalography and functional magnetic resonance imaging studies, little is known regarding the structural connectivity in CAE. We hypothesized that the structural connectivity would be disrupted in response to the decreased brain function in CAE.
Methods: Diffusion tensor imaging tractography was utilized to map the white matter (WM) structural network, composed of 90 cortical and sub-cortical regions, in 18 CAE and 18 age- and gender-matched healthy controls. Graph theoretical methods were applied to investigate the alterations in the topological and nodal properties of the networks in these patients.
Results: Both the CAE and the controls showed small-world properties in their WM networks. However, the network connection strength, absolute clustering coefficient, and global/local efficiency were significantly decreased, but characteristic path length was significantly increased in the CAE compared with the controls. Significantly decreased WM connections, nodal properties, and impaired sub-networks were found in the sub-cortical structures, orbitofrontal

* Corresponding author at: Key Laboratory for NeuroInformation of Ministry of Education, School of Life Science and Technology, University of Electronic Science and Technology of China, Chengdu, China. Tel.: +86 28 83201018; fax: +86 28 83208238.
E-mail address: dyao@uestc.edu.cn (D. Yao).
[1] Kaiqing Xue and Cheng Luo contributed equally to this work.

0920-1211/$ — see front matter
http://dx.doi.org/10.1016/j.eplepsyres.2013.10.002

area, and limbic cortex in the CAE. Moreover, network connection strength, local efficiency, and nodal features in some regions were significantly negatively correlated with the duration of epilepsy.

Conclusions: The present study demonstrated, for the first time, the disrupted topological organization of WM networks in CAE. The decreased connectivity and efficiency in the orbitofrontal and sub-cortical regions may serve as anatomical evidence to support the functional abnormalities related to the epileptic discharges observed in CAE. Moreover, the orbitofrontal sub-network may play a key role in CAE. These findings open up new avenues toward the understanding of absence epilepsy.

Introduction

Childhood absence epilepsy (CAE) is a non-convulsive, idiopathic, and generalized form of epilepsy, characterized by sudden and brief clinical consciousness impairment (several to many times per day) and accompanied by bilateral, synchronous, 2.5—4 Hz generalized spike wave discharges (SWDs) that can be observed using electroencephalography (EEG) (Crunelli and Leresche, 2002). The absence seizures generally start between 3 and 8 years old (peak manifestation of 6—7 years), and account for 10—17% of all types of childhood epilepsy (Crunelli and Leresche, 2002; Tenney and Glauser, 2013). Ethosuximide, valproic acid and lamotrigine are general initial monotherapy in CAE. Moreover, patients with CAE suffer from attention and executive impairment (Caplan et al., 2008), and the antiepileptic drugs may also lead to cognitive deficits (Glauser et al., 2010).

In recent studies, both the high temporal resolution of EEGs and the high spatial resolution of functional magnetic resonance imaging (fMRI) have been utilized to evaluate the mechanisms of SWDs in generalized epilepsy (Gotman et al., 2005; Bai et al., 2011; Luo et al., 2011a); and both interictal and ictal SWDs in CAE were associated with blood oxygen-level dependent (BOLD) signal changes in the basal ganglia-thalamocortical loop (Li et al., 2009). Functional connectivity based on fMRI has been widely used to study CAE. Abnormally increased functional connectivity was found in seizure-related regions, such as the orbitofrontal cortex, in patients with CAE (Bai et al., 2011). Decreased functional connectivity in the default mode network (DMN) was also found in patients with CAE, which suggests that the abnormalities in the DMN might be related to the cognitive mental impairment and unconsciousness experienced during absence seizures (Luo et al., 2011a). The functional connectivity of the human brain may be roughly predicted from structural connectivity (Honey et al., 2009). However, it is unclear what structural alterations are associated with the functional abnormalities observed in patients with CAE.

Diffusion tensor imaging (DTI), which is a non-invasive technology based on the principle that the magnitude and directionality of water diffusion is sensitive to the underlying brain microscopic tissue, such as the orientation and integrity of neural fibers (Beaulieu, 2002), has been widely used in studies of neurological and psychiatric disorders (Ciccarelli et al., 2008), such as schizophrenia (Ellison-Wright and Bullmore, 2009) and epilepsy (Luo et al., 2011b; Zhang et al., 2011b). The DTI-derived fractional anisotropy (FA) and mean diffusion (MD), a normalized ratio of diffusion orientation and the bulk mobility of water molecules, have been used predominantly to assess the microscopic tissue abnormalities observed in neurological and psychiatric disorders in most studies utilizing DTI (Pierpaoli and Basser, 1996). In particular, FA measures derived from DTI in humans in vivo were correlated with axonal membrane circumference (Concha et al., 2010). The association between the observation of DTI and histology in temporal lobe epilepsy patients implicated the application of DTI as a noninvasive marker of white matter pathology (Concha et al., 2010). Several studies have suggested a role for DTI in locating the epileptogenic zone in epilepsy (Eriksson et al., 2001; Rugg-Gunn et al., 2001; Assaf et al., 2003; Chen et al., 2008). DTI abnormalities were also found in white matter pathways in patients with juvenile myoclonic epilepsy (O'Muircheartaigh et al., 2012; Vollmar et al., 2012) and in rat absence epilepsy models (Chahboune et al., 2009). Moreover, structural connectivity using DTI tractography has been investigated for other generalized epilepsy syndromes (Liu et al., 2011; Zhang et al., 2011b; Kim et al., 2013).

Fiber tractography based on DTI is capable of visualizing the major fiber tracts in vivo to map the white matter (WM) network (Catani et al., 2002; Wakana et al., 2004). The complex WM network, in which nodes represent anatomical regions and edges represent the WM connections between pairs of nodes, can be adopted to describe the characteristics of generating and integrating information from multiple sources with high efficiency in human brain (Bullmore and Sporns, 2009). The WM network is also suitable for investigation of disorders lacking distinct radiological abnormality in the brain, such as schizophrenia (Zalesky et al., 2010) and CAE. The network parameters resulting from the graph theoretical method might provide valuable insights into the extent and nature of disturbances in the WM network. Graph theory is a powerful tool that quantitatively describes the features of complex systems, such as efficiency and small-world attribute (Sporns et al., 2004; Honey et al., 2007). Recently, Vaessen et al. (2012) found that impaired WM connectivity and the WM network topology were associated with cognitive comorbidities in patients with chronic temporal and frontal lobe epilepsy. These studies indicate that DTI can demonstrate structural abnormalities in patients with CAE, which would otherwise be missed with conventional neuroimaging.

Accordingly, the features of the WM network might reflect the alteration related to the epileptiform discharges and/or cognitive disturbance. In the present study, our primary hypothesis was that the topological characteristics

of the WM network are altered in patients with CAE. Furthermore, the local alterations in the WM network would be related to epileptic activity in patients. Therefore, we constructed and compared the WM structural connectivity network in patients with CAE with those of healthy volunteers.

Materials and methods

Subjects

Eighteen patients with CAE (all right-handed, 10 males and 8 females, age [mean ± SD] = 8.9 ± 2.1) were recruited from the Neurology Department of the West China Hospital, Sichuan University. The diagnoses for each patient were established according to the recommendations of the International League Against Epilepsy (ILAE) (Engel, 2001). Recruitment was based on the following criteria: (i) All patients underwent a 24-h video electroencephalogram with 18 channels, and at least two epochs of seizures were captured during the monitoring; and (ii) no focal abnormalities were found during routine structural MRI examinations. Eighteen age- and gender-matched healthy controls (all right-handed, 10 males and 8 females, age [mean ± SD] = 8.5 ± 1.8), who had no history of neurological or psychiatric disorders and no obvious abnormalities during a routine MRI examination, were recruited. There were no significant differences in age or gender between the two groups (two sample two-tailed t-test for age, $p = 0.563$; χ^2 test for gender, $p = 1.0$).

After a full explanation, written informed consent was obtained from all of the subjects and their parents. The study was approved by the medical ethical committee at West China Hospital, Sichuan University.

Data acquisition

MRI data were collected using a 3.0 T scanner (EXCITE, GE, Milwaukee, WI, USA) with an eight-channel-phased array head coil. All subjects were instructed to rest their eyes (closed) and to minimize their head movements. First, anatomic 3D-T1-weighted axial images were acquired using a spoiled gradient recall (SPGR) sequence that covered the entire brain (156 slices, TR = 8.5 ms, TE = 3.4 ms, matrix = 512 × 512, FOV = 24 cm × 24 cm, flip angle = 12°). Second, the DTI acquisition used a single-shot spin-echo planar imaging sequence (TR = 10, 000 ms, TE = 79.7 ms, NEX = 2, matrix = 256 × 256, FOV = 24 cm × 24 cm, thickness = 3 mm without gaps, 50 slices covered the whole brain). One unweighted ($b = 0\,s/mm^2$) and 15 diffusion-weighted ($b = 1000\,s/mm^2$, non-collinear gradient directions) image volumes were collected.

Data preprocessing

For each subject, the T1-weighted data and the DTI data were visually examined by 2 radiologists to exclude any subjects with obvious head motions and rock-ribbed artifacts. Subsequently, the 15 diffusion-weighted scans were aligned to the first unweighted B0 image ($b = 0\,s/mm^2$) to minimize slight head movements using the SPM8 software package (Statistical Parametric Mapping, http://www.fil.ion.ucl.ac.uk/spm/software/spm8). We also evaluated the group differences in translation and rotation of head motion. The results showed that there were no significant differences between the two groups (see Supplementary Material I).

Supplementary material related to this article can be found, in the online version, at http://dx.doi.org/10.1016/j.eplepsyres.2013.10.002.

Eddy current distortions existing in the diffusion-weighted image volumes were corrected by affine registration to the reference B0 images.

Network construction

Nodes (or vertices) and edges (arcs) are two fundamental elements of a network (Rubinov and Sporns, 2010). In the current study, a network composed of 90 nodes and a quantity of WM connectivity edges linking these nodes was constructed using the following procedures for each subject. Fig. 1 shows the whole process used for the construction of a network in the human brain using DTI tractography.

Network node definition

The procedure used for defining the nodes of the network for each subject was the same as described in previous studies (Gong et al., 2009; Shu et al., 2011; Bai et al., 2012). First, each individual T1-weighted structural image was co-registered to its B0 image ($b = 0\,s/mm^2$) in the DTI native space, using a linear transformation. Second, the co-registered structural images in the DTI native space were registered to the ICBM-152 T1 template in the MNI space to obtain an affine transformation matrix, T, with 12 degrees of freedom, together with a series of non-linear warps characterized by a set of $7 \times 8 \times 7$ basis functions. Finally, the inverse transformation matrix T^{-1} was utilized to warp the automated anatomical labeling (AAL) atlas (Tzourio-Mazoyer et al., 2002), which has been used in several previous studies (Achard et al., 2006; Iturria-Medina et al., 2008), from the MNI space to the DTI native space. The procedure preserved discrete labeling values using the nearest-neighbor interpolation method in the SPM8 package. After the above procedure, the cerebral cortex and sub-cortex for each subject were anatomically parcellated into 90 regions of interest (ROI), 45 for each hemisphere, with the regions of the cerebellum being excluded (see Table 1). Each ROI represents one node of the WM anatomical structural network in a subject.

White matter fiber tractography

The corrected diffusion-weighted images and $b = 0$ image were used to reconstruct the whole brain white matter tracts for each subject. The diffusion tensor was estimated by the linear least-squares fitting method at each voxel, using the interactive software Diffusion Toolkit 0.6.2 (http://trackvis.org/dtk/, Wang et al., 2007), and whole brain fiber tracking was performed in the DTI native space. During tracking, the FACT (fiber assignment by continuous tracking) algorithm was employed (Mori et al., 1999). If the FA value was lower than 0.15 or the angle between the current and the previous path segment was higher than 35

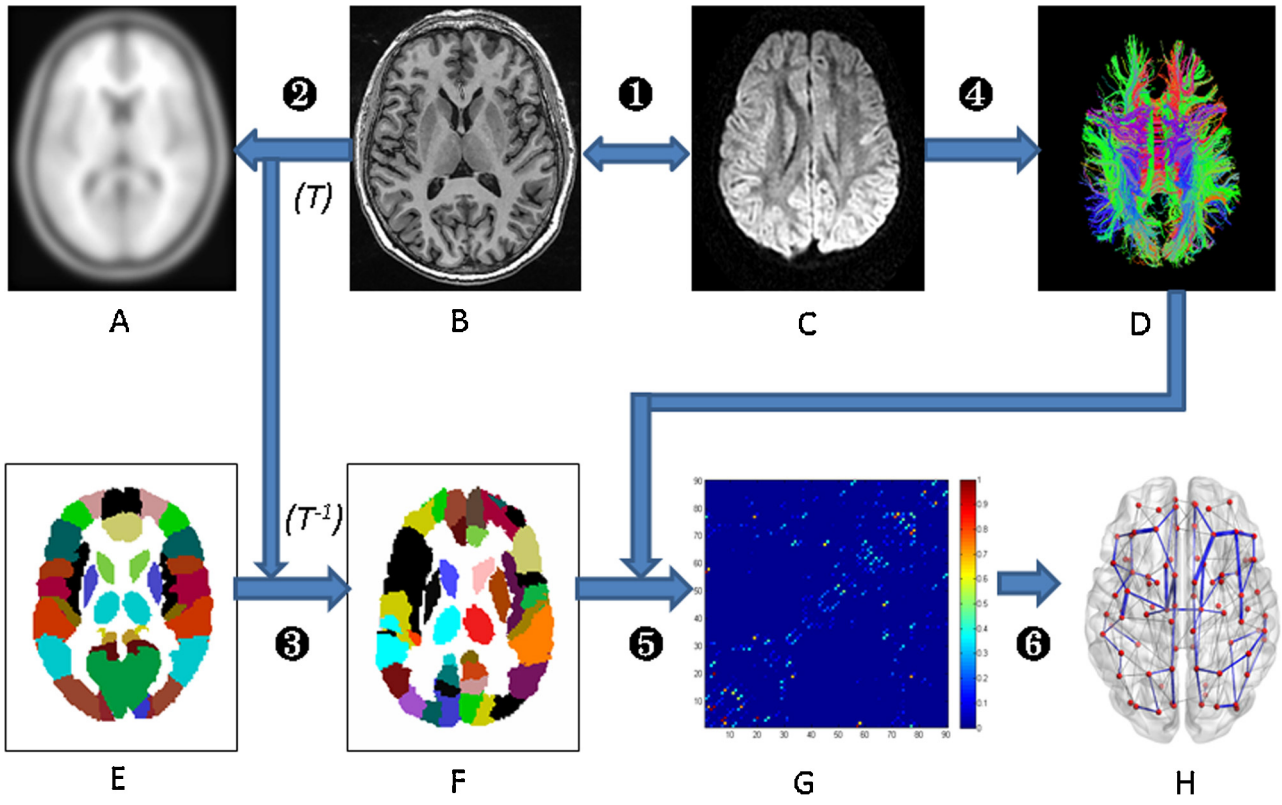

Figure 1 A flowchart for the construction of an anatomical network in the human brain using DTI. (A) The T1 template of ICBM152 in the MNI space. (B) A structural MRI in the DTI space. (C) A weighted diffusion tensor image. (D) The estimated whole brain fiber trajectories. (E) An AAL template in the MNI space. (F) A subject-specific AAL mask in the DTI space. (G) The whole brain network matrix. (H) A 3D-visualization of the backbone network. The processing program worked as follows: step 1, the structural MRIs in the DTI space were registered to the T1 template in the MNI space; step 2, a transformation matrix was obtained, T; step 3, the inverse transformation matrix T^{-1} was used on the AAL template in the MNI space to generate the subject-specific AAL mask in the DTI native space; step 4, the fibers in whole brain were reconstructed using deterministic tractography; step 5, a whole brain anatomical network matrix was produced according to any two regions of the AAL mask and the fibers between them; and step 6, the backbone was extracted from the above matrix and its visualization.

degrees, the path tracking was stopped. After whole fiber tracking, any fiber shorter than 20 mm or longer than 300 mm and obvious false paths were discarded (Liao et al., 2011). To ensure that each brain region was sufficiently in contact with the fibers, they were expanded 2—3 mm into the white matter. Fiber bundles connecting each pair of brain regions were extracted from the total collection of brain fibers.

Network edge definition

Two regions (region i and region j) were considered structurally connected if at least one fiber bundle with two endpoints was located in these two regions (Liao et al., 2011; Bai et al., 2012). According to the number of fibers linking region i and region j, the weight of the edge linking regions i and j was defined as:

$$w(i,j) = \frac{N_{i,j}}{\max(N_{i,j})} \quad i,j = 1,2,3\ldots 90, i \neq j,$$

where $N_{i,j}$ is the number of fibers linking region i and j, and $\max(N_{i,j})$ is the maximum number of fibers linking any two nodes in a graph G.

After the above procedure, a weighted WM network, represented in a symmetric 90×90 matrix, was constructed for each subject.

Connectivity backbone

Because of noise and limitations in deterministic tractography, the risk of false-positive connections exists. To limit this risk, a connectivity backbone was estimated according to the above-mentioned network for each subject (Hagmann et al., 2008; Iturria-Medina et al., 2011). In detail, first, a maximum spanning tree, which connects all nodes of the network such that the sum of its weights is maximal and in which there are no cycles, was extracted. Then, additional edges were added in order of their weights until the average node degree (the degree of a node is the number of edges connected to that node in a graph) was K. To insure the sparseness and efficiency of the network, the K was set as 4 according to our previous experience (Iturria-Medina et al., 2011) and a previous study (Hagmann et al., 2008). All subsequent network (Graph) analyses and visual representations were based on the resultant network (connectivity backbone).

Table 1 Cortical and subcortical regions defined in AAL template in standard stereotaxic space.

Region name	Abbreviation	Region name	Abbreviation
Superior frontal gyrus, dorsolateral	SFGdor	Superior occipital gyrus	SOG
Superior frontal gyrus, orbital	SFGorb	Middle occipital gyrus	MOG
Superior frontal gyrus, medial	SFGmed	Inferior occipital gyrus	IOG
Superior frontal gyrus, medial orbital	SFGmorb	Fusiform gyrus	FG
Middle frontal gyrus	MFG	Superior parietal gyrus	SPG
Middle frontal gyrus, orbital	MFGorb	Paracentral lobule	PCL
Inferior frontal gyrus, opercular	IFGoper	Postcentral gyrus	PoCG
Inferior frontal gyrus, triangular	IFGtri	Inferior parietal gyrus	IPG
Inferior frontal gyrus, orbital	IFGorb	Supramarginal gyrus	SMG
Rectus gyrus	REG	Angular gyrus	ANG
Anterior cingulate gyrus	ACC	Precuneus	PCNU
Olfactory cortex	OLF	Posterior cingulate gyrus	PCC
Precentral gyrus	PreCG	Superior temporal gyrus	STG
Supplementary motor area	SMA	Superior temporal gyrus, temporal pole	STGp
Rolandic operculum	ROL	Middle temporal gyrus	MTG
Median-and para-cingulate gyrus	MCC	Middle temporal gyrus, temporal pole	MTGp
Calcarine fissure and surrounding cortex	CAL	Inferior temporal gyrus	ITG
Cuneus	CUN	Heschl gyrus	HES
Lingual gyrus	LING	Parahippocampal gyrus	PHIP
Thalamus	THA	Insula	INS
Caudate nucleus	CAU	Hippocampus	HIP
Lenticular nucleus, putamen	PUT	Amygdala	AMYG
Lenticular nucleus, pallidum	PAL		

Graph theory analysis

In the current study, to characterize the topological organization of WM networks at the global and regional levels, we used the Brain Connectivity Toolbox (http://www.brain-connectivity-toolbox.net) (Rubinov and Sporns, 2010) to analyze the following graph measures: weighted network connectivity strength, clustering coefficient, path length, global efficiency, local efficiency, nodal efficiency and small-world property.

Connectivity strength

For a weighted graph (network), G, with N nodes and K edges, connectivity strength (S_i) is defined as the sum of the edge weights, w_{ij}, directly linked to node i. Formally:

$$S_i = \frac{1}{N}\sum_{i \in G} w_{ij}.$$

The larger S_i is, the more important node i becomes. The network strength (S_P) is the average of all strengths across all nodes in the graph G:

$$S_P = \frac{1}{N}\sum_{i \in G} S_i.$$

S_P is the measure used to evaluate the degree of connectivity strength over the whole network.

Clustering coefficient

In a weighted graph, G, the absolute clustering coefficient of a node, i, is defined as the geometric average of the subgraph node weights (Onnela et al., 2005):

$$C_i = \frac{1}{k_i(k_i-1)} \sum_{\substack{j,k \in G \\ j,k \neq i}} (w_{ij} \cdot w_{jk} \cdot w_{ki})^{1/3},$$

where k_i is the number of edges linking a node, i (i.e., the degree of node i), and w is the weight of an edge connecting two nodes. If a node is isolated or has just one connection, i.e., $k_i = 0$ or $k_i = 1$, the clustering coefficient of node i is zero, $C_i = 0$. The absolute clustering coefficient of a graph, G, is the average of the absolute clustering coefficient over all nodes:

$$C_P = \frac{1}{N}\sum_{i \in G} C_i.$$

C_P is a measure of the extent of the local interconnectivity or cliquishness in a graph (Watts and Strogatz, 1998; Latora and Marchiori, 2001).

Path length

The path length between two nodes, i and j, is defined as the sum of the edge lengths along the path, where each edge length was obtained by calculating the reciprocal of the edge weight value, $1/w_{ij}$. The shortest path length (L_{ij}) between two nodes, i and j, is the minimum sum of the edge weights among all paths from node i to node j. The

characteristic path length (L_P) of a weighted graph is defined as a ''harmonic mean'' length between pairs (Newman, 2003), that is, the reciprocal of the average of the reciprocals:

$$L_P = \frac{1}{1/(N(N-1))\sum_{j \neq i \in G} 1/L_{ij}}.$$

This definition solves the problem of L_{ij} becoming infinite when nodes i and j are located in two non-interconnected components of a graph. L_P quantifies the ability of a network to propagate information in parallel. A larger L_P correlates with a worsened ability to propagate information in parallel.

Global efficiency

The global efficiency (E_{global}) can be calculated as (Latora and Marchiori, 2001):

$$E_{global} = \frac{1}{N(N-1)} \sum_{i \neq j \in G} \frac{1}{L_{ij}},$$

where L_{ij} is the shortest path length between nodes i and j in graph G. The global efficiency is the reciprocal of the characteristic path length of a weighted network, i.e., $E_{global} = 1/L_P$; therefore, in terms of the information flow, the global efficiency of a network, similar to the characteristic path length, reflects how efficiently information can be exchanged over the whole network. A larger E_{global} correlates with a more powerful efficiency.

Local efficiency

The local efficiency of the node i is calculated as (Latora and Marchiori, 2001):

$$E_{local} = \frac{1}{N} \sum_{j \neq k \in G} E_{global}(G_i),$$

where G_i is the subgraph of the first neighbors of node i (i.e., the set of nodes that are the direct neighbors of node i). This measure has been used to reveal the fault tolerant capability of a system, showing how efficient the communication is among the first neighbors of node i when i is removed.

Nodal efficiency

The nodal efficiency for a given node i (E_i) was defined as the reciprocal of the harmonic mean of the shortest path length between node i and all other nodes in the network (Achard and Bullmore, 2007):

$$E_i = \frac{1}{(N-1)} \sum_{i \neq j \in G} \frac{1}{L_{ij}},$$

where L_{ij} is the shortest path length between node i and node j. The nodal efficiency quantifies the importance of the nodes for communication within the network. The nodes with high nodal efficiencies can be categorized as hubs in a network (Achard and Bullmore, 2007).

Small-world property

The normalized clustering coefficient γ and the normalized characteristic path length λ of a network are defined as (Watts and Strogatz, 1998):

$$\gamma = \frac{C_P^{real}}{C_P^{rand}} \text{ and } \lambda = \frac{L_P^{real}}{L_P^{rand}},$$

where C_P^{real} and L_P^{real} represent the clustering coefficient and the characteristic path length of a real network, respectively. C_P^{rand} and L_P^{rand} are, respectively, the mean clustering coefficient and the characteristic path length of 1000 random networks that preserve the same number of nodes, edges, and degree distributions as the real network (Sporns et al., 2004). If a network has a similar path length but a higher clustering coefficient, that is $\gamma \gg 1$ and $\lambda \approx 1$, then the network is a small-world network (Watts and Strogatz, 1998). Furthermore, the above two conditions can also be summarized into a scalar quantitative measurement, the small-worldness: $\sigma = \gamma/\lambda$. Consequently, if $\sigma > 1$, the network has a small-world property (Achard et al., 2006).

Statistical analyses

Based on the WM network constructed for each subject, we performed statistical comparisons of the WM connection strengths, network characteristics, and nodal properties between the patients with CAE and healthy controls. In addition, the significantly different sub-network components between the two groups were identified. Of note, the effects of age and gender were adjusted for all of the analyses.

Comparisons of WM connections

To determine the impaired WM connections in patients with CAE, a univariate analysis of covariance (ANCOVA) was performed on the subset of all pairs of nodes (regions) within the two groups ($p < 0.05$, FDR corrected). The subset was composed of consistent connections that were determined by analyzing each pair of brain regions across all subjects using a nonparametric one-tailed sign test ($p < 0.05$, Bonferroni corrected) (Gong et al., 2009). This constraint ensured that any compared connection existed in most subjects and the subset would be used in network-based statistic.

Comparisons of network characteristics

To determine the group differences in global network characteristics (S_P, C_P, L_P, E_{local}, E_{global}, γ, λ, σ), statistical comparisons were performed between the two groups using a univariate ANCOVA ($p < 0.05$, Bonferroni corrected), respectively.

Comparisons of nodal properties

Three regional nodal properties (S_i, C_i, E_i) were also statistically compared between the two groups, across all 90 nodes using a univariate ANCOVA ($p < 0.05$, FDR corrected).

Network-based statistic

Network-based statistic (NBS) is a nonparametric statistical test used to isolate the components (sub-networks, a set of interconnected edges) of an $N \times N$ undirected adjacency

Table 2 Main clinical information for 17 patients with CAE.

No.	Gender	Age	Age of onset	Frequency of seizure	Antiepileptic drugs	Frequency of SWDs (Hz)
1	M	10	5	2—3/d	None	2.5—3.5
2	M	7	4	15/d;	VPA	3—3.5
3	M	11	9	7—8/d	None	3
4	M	5	2	several/d	None	3
5	F	9	4	20/d	None	3
6	M	8	6	18/d	None	3
7	F	10	9	several/d	TCM, VPA	2—3
8	M	8	6	several/d	None	2.5—3.5
9	F	7	4	several/d	None	3
10	M	8	6	several/d	None	2.5—3
11	F	12	9	2—5/d	VPA	3.5
12	F	6	4	several/d	None	3
13	M	11	6	several/d	None	3.5
14	M	9	6	3—6/d	None	3—3.5
15	F	12	7	several/d	VPA	3
16	M	10	6	8—9/d	None	3.5
17	F	11	9	several/d	None	3

M, male; F, female; d, day; VPA, valproic acid; TCM, traditional Chinese medicine.

matrix that differs significantly between two distinct populations (Zalesky et al., 2010, 2012). NBS has been applied successfully in studies of schizophrenia (Zalesky et al., 2010), major depressive disorder (Zhang et al., 2011a), and other disorders (Bai et al., 2012). In the current study, we used NBS to identify the significantly different sub-networks of patients with CAE. First, the subset that produced in comparisons of WM connections was considered as the connection mask. Second, the most consistent connections for each subject in the two groups were detected. Finally, the NBS software (http://www.nitrc.org/projects/nbs/) was conducted within the consistent connections, in which the t-value was set at 2.5 and permutation times at 10,000, according to our experience and previous studies (Zalesky et al., 2010; Bai et al., 2012; Wang et al., 2013). For a detailed description of the NBS approach, see the study by Zalesky et al. (2010).

Relationship between network topological indices and duration of epilepsy

To evaluate the relationship between the duration of epilepsy and the topological indices (S_P, C_P, L_P, E_{local}, E_{global}, γ, λ, and σ) of WM networks in patients with CAE, a partial correlation analysis was employed, controlling for age and gender as nuisance covariates ($p < 0.05$, Bonferroni corrected). Moreover, we also evaluated the relationship between the duration of epilepsy and the altered nodal properties (S_i, C_i, and E_i) of WM networks in patients with CAE by the same methods.

Results

The DTI data of one patient were eliminated because of predominant motion artifacts. The main clinical information for the remaining 17 patients is summarized in Table 2.

Differences of WM connections between groups

In contrast to healthy controls, 17 pairs of WM connections exhibited a significant decrease in CAE ($p < 0.05$, FDR corrected), and no increased WM connection were found. These connections were three-dimensionally visualized using the BrainNet Viewer software (NKLCNL, www.nitrc.org/projects/bnv) (Fig. 2). In detail, four of these connections, which are highlighted with blue lines in Fig. 2, were associated with the orbitofrontal cortex. Eight connections were associated with the sub-cortical structures or the limbic system and are shown by black lines in Fig. 2. The remaining five connections were associated with other cortexes and are highlighted with green lines in Fig. 2.

Differences in network characteristics between groups

The network connection strength (S_P), the absolute clustering coefficient (C_P), the local efficiency (E_{local}), and the global efficiency (E_{global}) were significantly decreased in the CAE, and the characteristic path length (L_P) was significantly increased in the CAE compared with the healthy controls ($p < 0.05$, Bonferroni corrected). For the small-world properties (γ, λ, and σ), the σ was greater than one in both groups, which indicates that both groups showed small-world architecture in the brain structural networks. However, no significant changes were observed in γ, λ, or σ. The details are shown in Fig. 3.

Differences in nodal properties between groups

In contrast to healthy controls, the pattern of nodal properties was significantly decreased in some brain regions in CAE ($p < 0.05$, FDR corrected). In detail, decreased connectivity strength was found in 11 regions, such as the bilateral orbital

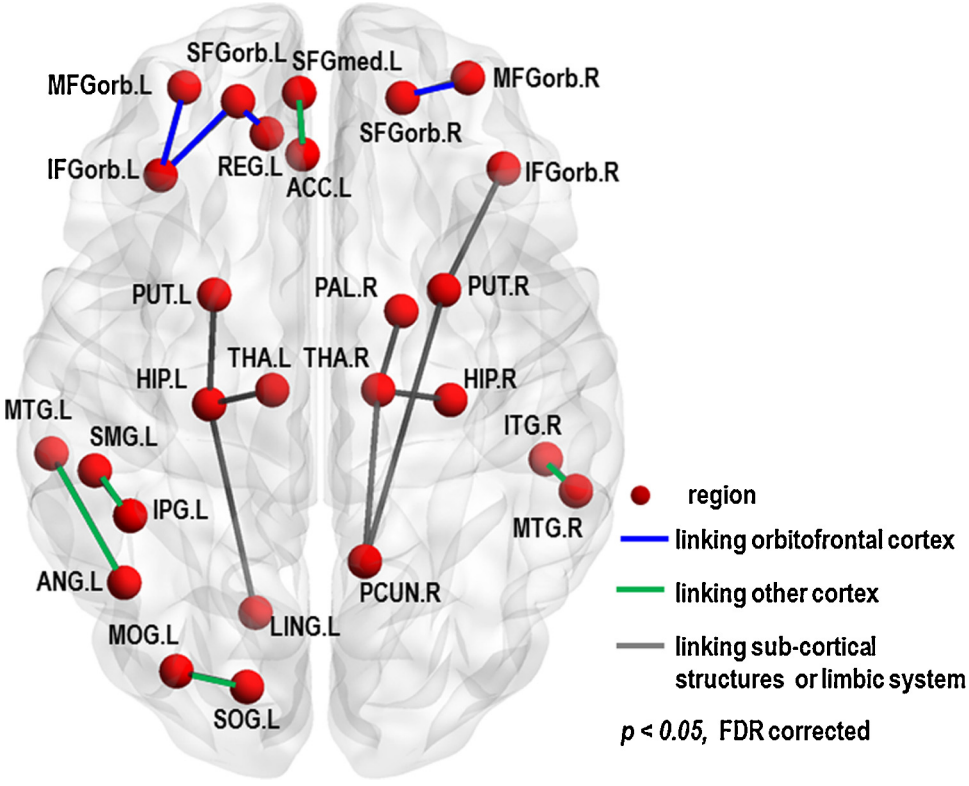

Figure 2 Connection comparisons between the CAE and HC groups. Seventeen pairs of regions exhibited significantly decreased connectivity in CAE patients compared to health controls ($p < 0.05$, FDR corrected). Four connections were associated with the orbitofrontal cortex, eight connections were associated with the sub-cortical structures or limbic system and the other five decreased connections were related with other cortexes. These connections were three-dimensionally visualized using the BrainNet Viewer software (NKLCNL, www.nitrc.org/projects/bnv). For abbreviations of region names, see Table 1.

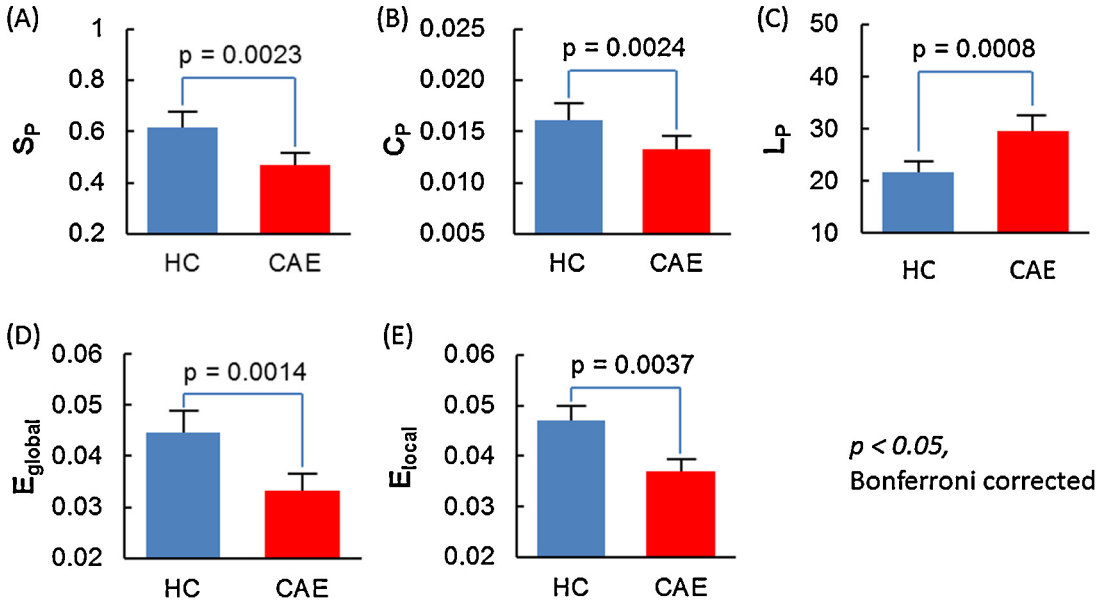

Figure 3 Network topological properties and small-world properties. The connectivity strength S_P, mean clustering coefficient C_P, global efficiency E_{global}, and local efficiency E_{local} were significantly reduced in the CAE group compared with the HC group The characteristic path length L_P was longer in the CAE group than the HC group ($p < 0.05$, Bonferroni corrected).

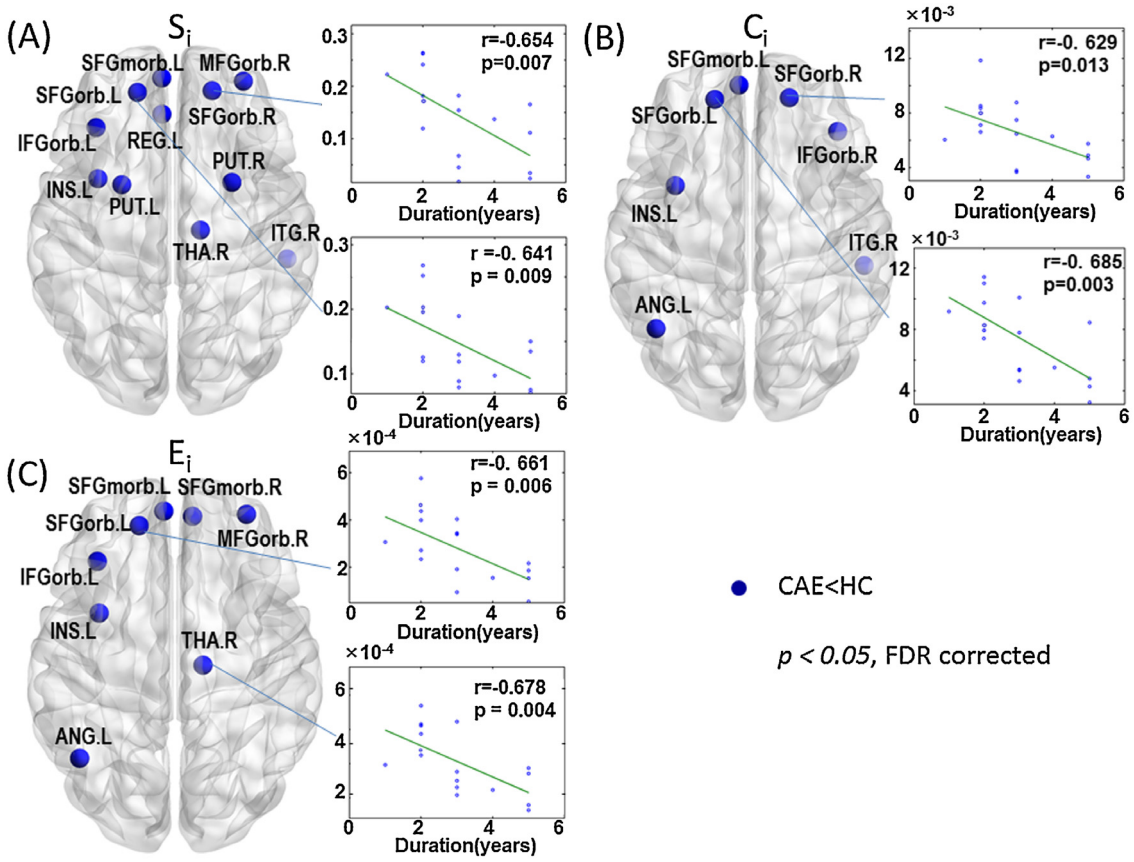

Figure 4 The Distribution of regions with significantly altered nodal properties in patients with CAE relative to healthy controls and the relationship between altered nodal properties and the duration of epilepsy. (A) The group differences in nodal connectivity strength S_i, (B) the nodal clustering coefficient C_i and (C) the nodal efficiency E_i are presented in three-dimensional rendering maps. Blue spheres denote the regions with significantly decreased nodal characteristic in CAE patients ($p < 0.05$, FDR corrected). The relationship between the nodal characteristics and the duration of epilepsy in CAE patients is shown in the scatter plots. The significantly different regions all show decreased nodal characteristics in CAE patients, and no node shows a positive correlation with epilepsy ($p < 0.05$, FDR corrected). For abbreviations of region names, see Table 1.

region of the superior frontal gyrus, the left orbital region of the inferior frontal gyrus, and the right putamen (Fig. 4A). A decreased clustering coefficient was found in seven regions, such as the bilateral orbital region of the superior frontal gyrus, and the left medial orbital region of the superior frontal gyrus (Fig. 4B). A decreased nodal efficiency was found in eight regions, such as the bilateral medial orbital region of the superior frontal gyrus, the left orbital region of the superior frontal gyrus, and the right thalamus (Fig. 4C). No increased structural connections were found in CAE.

Sub-networks Isolated by NBS

NBS is used to isolate the components of an $N \times N$ undirected connectivity matrix that differ significantly ($p < 0.05$, corrected) between two groups The results revealed three disconnected sub-networks in CAE compared with healthy controls (Fig. 5). The first component was composed of 4 nodes (the left orbital region of the superior frontal gyrus, the left orbital region of the middle frontal gyrus, the left orbital region of the inferior frontal gyrus, and the left rectus gyrus), and 3 connections in the left orbitofrontal cortex showed a decrease in CAE ($p = 0.005$, corrected). The second component was composed of 4 nodes (the left thalamus, the left putamen, the left hippocampus, and the left lingual gyrus), and 3 connections showed decreased connectivities in CAE ($p = 0.003$, corrected). The third component was composed of 5 nodes (the right thalamus, the right hippocampus, the right putamen, the right precuneus, and the right pallidum), and 3 connections in the right sub-cortical structures showed decreased connections in CAE ($p = 0.005$, corrected). All three sub-networks showed decreased mean connectivity values in the CAE compared to the healthy controls (for a visualization of these results, see Fig. 5).

Relationships between the altered topological indices and duration of epilepsy

The relationships between the duration of epilepsy and the topological indices of WM networks were evaluated. Controlling the age and gender effects, two topological indices (S_P and E_{local}) of WM networks in CAE were significant negative correlated with the duration of epilepsy ($p < 0.05$, Bonferroni corrected, Fig. 6). Moreover, the nodal features (S_i, C_i, and

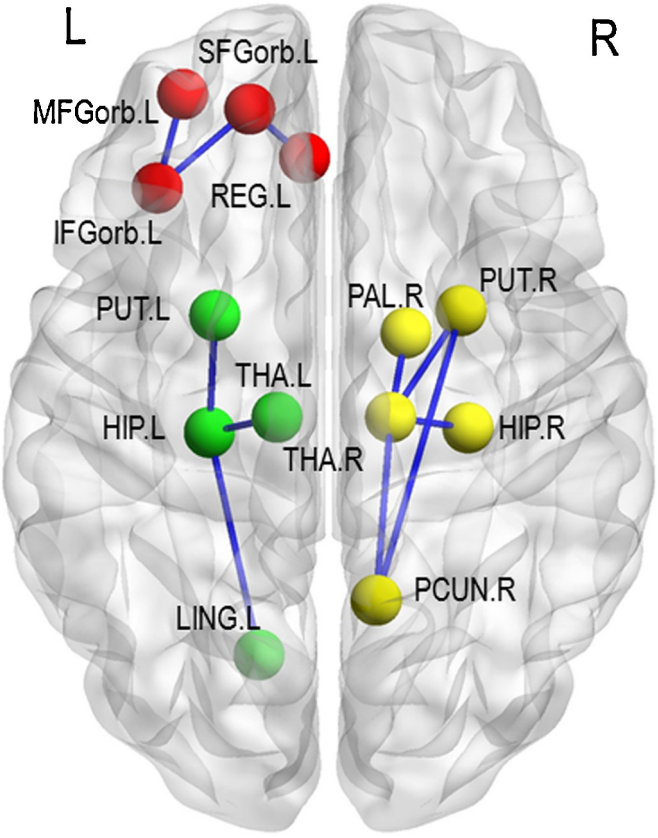

Figure 5 The three disconnected components identified in CAE patients. (A) The component composed of four orbitofrontal nodes (SFGorb.L, MFGorb.L, IFGorb.L and REG.L) and three decreased connections in CAE patients ($p = 0.005$, corrected). (B) The component composed of four subcortical nodes (THA.R, HIP.R, PUT.R PCUN.R and PAL.R) and five decreased connections in CAE patients ($p = 0.003$, corrected). (C) The component composed of four subcortical-limbic and association cortex nodes (THA.L, HIP.L, MTG_P.L and LING.L) and three decreased connections in CAE patients ($p = 0.005$, corrected). All three sub-networks were decreased in the CAE patients. For abbreviations of region names, see Table 1.

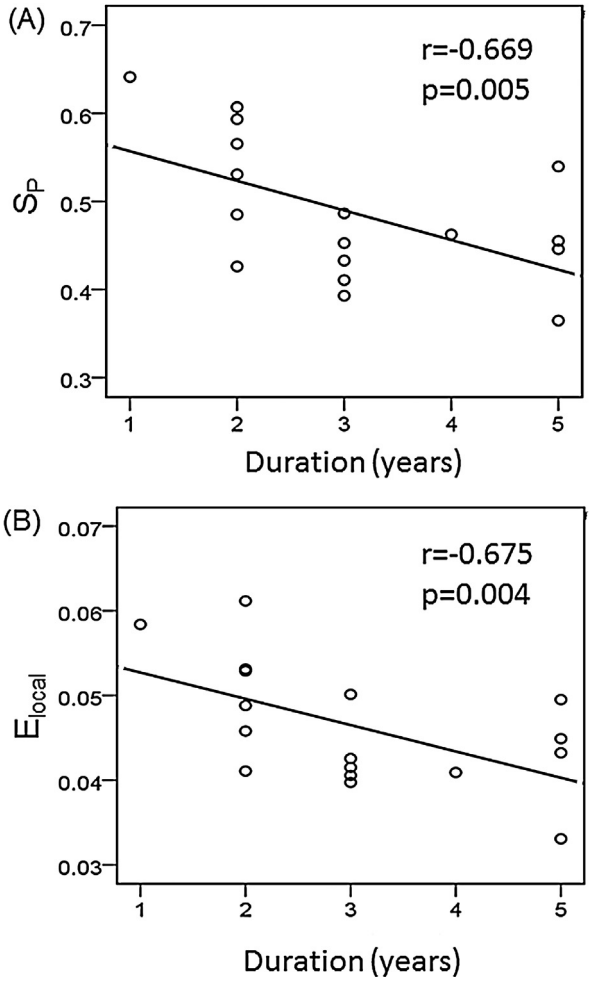

Figure 6 The relationship between the topological properties (S_P and E_{local}) of structural connectivity networks and the duration of epilepsy. Significant negative correlations were found between both (A) S_P ($r = -0.669$, $p = 0.005$) and (B) E_{local} ($r = -0.675$, $p = 0.004$) and the duration of epilepsy.

E_i) in the some orbitofrontal regions were negatively correlated with the duration of epilepsy ($p < 0.05$, FDR corrected, Fig. 4).

Discussion

To the best of our knowledge, this is the first study devoted to the identification of WM network alterations in CAE. Individual networks were created by means of fiber tractography, and graph theoretical tools were used to analyze their features. Compared with healthy controls, three primary differences were observed in CAE: first, the organization of the WM network in CAE was significantly disrupted, as indicated by reduced network strengths, clustering coefficients, and local and global efficiencies and longer characteristic path lengths; second, decreased regional characteristics and connections were observed in orbitofrontal, limbic, occipital lobe, and sub-cortical structures; finally, three impaired sub-networks were found in the orbitofrontal and sub-cortical structures, which might reflect the altered structural pathway in the basal ganglia-thalamo cortex that is implicated in the core circle for the generation and propagation of SWDs in CAE.

Disrupted overall topology of WM networks

Although previous studies have suggested that absence epilepsy may be a disorder resulting from the abnormal connectivity of brain functional networks (Crunelli and Leresche, 2002; Bai et al., 2011), little is known regarding the underlying anatomic structural substrates responsible for these functional abnormalities. In the current study, the WM networks for both groups showed a small-world architecture, which was consistent with the previous functional connectivity studies performed examining various types of epilepsy (Ponten et al., 2007; Shehata and Bateh, 2009; Liao et al., 2010; Bernhardt et al., 2011; Zhang et al., 2011b). Several topological properties, however, were significantly decreased in CAE, including reduced network connectivity strengths, clustering coefficients, and local and global

efficiencies, as well as a longer characteristic path length. The reduced network connectivity strengths and clustering coefficients were related to the sparse connectivity of the networks, which might suggest reduced white matter integrity in CAE. Together with the longer path length and the reduced local and global efficiencies, these findings not only demonstrated the sparse connectivity in WM networks but also indicated the disorganization and reduced efficiency of WM networks in CAE. Crucially, we found that two topological indices (S_P and E_{local}) of WM networks in CAE were negatively correlated with the duration of epilepsy. Prolonged exposure to epileptiform discharges might impair the white matter fibers and induce reduced connectivity strengths and local efficiencies. These alterations might provide new insights into understanding the underlying structural substrates of abnormal functional connectivity in patients with CAE.

White matter network abnormalities related to epileptic activity

Even though the current general view is that the brain structure in CAE is normal, based on conventional MRI studies, some studies have revealed abnormalities in volume and diffusion parameters in CAE. In our previous studies, we not only found decreased volumes in the basal ganglia and thalamus but also identified an abnormality in the diffusion parameters of the basal ganglia, thalamus, and some cortical regions (Luo et al., 2011b; Yang et al., 2012). Caplan and her colleagues also found volume reductions in the orbitofrontal gyrus and temporal lobe and suggested that disturbances in these regions supported the cortical focus theory of CAE (Caplan et al., 2009). In the current DTI study, we found decreased WM connectivity attributes in the orbitofrontal cortex, including decreased nodal strength, clustering coefficient, and efficiency. The NBS analysis showed also a decreased subnetwork in the orbitofrontal cortex. In a previous EEG study, the orbitofrontal and medial frontal regions were considered to be key regions related to the generation of SWDs (Tucker et al., 2007). Moreover, the frontal lobe showed earlier BOLD signal changes related to the SWDs during simultaneous EEG and fMRI recordings (Carney et al., 2012). Recently, abnormal functional connectivity related to the orbitofrontal cortex was found in CAE based on resting state fMRI (Bai et al., 2011). In the present study, the decreased nodal strength and efficiency observed in the orbitofrontal cortex might provide additional evidence to support an orbitofrontal cortex abnormality in CAE. Moreover, the disrupted local properties of some nodes in the orbitofrontal cortex were gradually associated with increased duration of epilepsy. We presume that the WM network abnormalities in the orbitofrontal cortex might be related to the generation of SWDs in CAE. The sub-network composed of the orbitofrontal cortex nodes may be considered to be a key network for epileptic activity in CAE. More functional imaging methods, such as simultaneous EEG and fMRI, should be utilized to uncover impairments in the orbitofrontal cortex during SWDs in the future to confirm the role of this sub-network in CAE.

The sub-cortical nuclei were thought to play an important role in the generation and propagation of SWDs in CAE, especially the basal ganglia-thalamocortical circuit (Crunelli and Leresche, 2002). In our previous studies, we found structural abnormities in the basal ganglia and thalamus (Luo et al., 2011b) and identified abnormal functional connectivities in the basal ganglia network in CAE (Luo et al., 2012). The previous findings were concordant with the suggested impairment of the basal ganglia-thalamocortical circuit based on structural and functional imaging in CAE. Here, some decreased structural connections among the sub-cortical nuclei (e.g., thalamus-pallidum, thalamus-hippocampus, and putamen-hippocampus) and between the sub-cortical nuclei and cortical regions (e.g., putamen-precuneus, thalamus-precuneus, and hippocampus-temporal pole) were also found in CAE. Abnormal sub-networks were also found to be related to the sub-cortical nuclei, and some cortical nodes were also included (left lingual gyrus and right precuneus). The current results are consistent with previous studies and might serve as the potential structural foundation for the differences found in functional neuroimaging studies.

The cortical regions have also been reported to be associated with absence epilepsy (Bai et al., 2011; Luo et al., 2011a). Here, abnormal structural connectivity was also found in cortical regions. First, some nodes, which were commonly identified using the DMN in previous studies (Liao et al., 2011; Qi et al., 2012), were found to have abnormal nodal properties, such as decreased clustering coefficients in the angular gyrus and inferior temporal gyrus, reduced strength in the inferior temporal gyrus, and decreased nodal efficacy of the angular gyrus. The DMN was identified as a resting state of brain function (Raichle et al., 2001). In simultaneous EEG-fMRI studies, a deactivation related to interictal generalized epileptic discharges was found in the DMN (Gotman et al., 2005; Li et al., 2009). Moreover, an abnormal resting state functional connectivity in the DMN was also observed in absence epilepsy (Bai et al., 2011; Luo et al., 2011a). The disturbed nodal parameters of the WM network in these regions were consistent with previous functional studies (Luo et al., 2012), which might reflect the anatomic abnormality of the functional findings in the DMN. Second, the occipital nodes were identified. The occipital lobe has rarely been mentioned in previous studies of CAE. Recently, a MEG study revealed occipital precursor activity with a low frequency of SWDs in CAE (Gupta et al., 2011). However, the occipital area in CAE needs to be assessed with a larger data set. Some decreased structural connections and regions with decreased nodal parameters were found in the association cortex. One recent study in temporal and frontal lobe epilepsy found impaired WM connectivity and network topology, which suggested that the abnormality might reflect the cognitive disturbance in patients with chronic epilepsy (Vaessen et al., 2012). Although neuropsychological testing was not performed in the current study, the cognitive and behavioral deficits associated with CAE have been observed in previous studies (Pavone et al., 2001; Henkin et al., 2005; Vaessen et al., 2012). In the current study, the impairment in these association cortex nodes might be related to the cognitive and behavioral deficits in CAE as a result of the structural defects.

Limitations and methodological issues

The authors acknowledge several limitations and methodological issues regarding the present study. First, the effects of antiepileptic drugs should be considered. The results could be affected by a variety of antiepileptic drugs, such as valproic acid and traditional Chinese medicine, which can affect normal neuronal function and produce cognitive impairments (Kwan and Brodie, 2001; Ortinski and Meador, 2004). However, it was not possible to control for the heterogeneous effects of various anti-epileptic drugs in our design. Second, the parameters of DTI acquisition might influence the findings. The number of orientations ($n = 15$ in the current study) might affect the robustness to estimate the anisotropy of diffusion (Jones, 2004). The non-cubic voxel in DTI data was also limitation because an isotropic resolution may facilitates the fiber tracking (Basser et al., 2000). These parameters will be optimized in future studies. Third, a deterministic tractography method was employed to define the edges of the WM networks. Although this method has been used in previous studies (Gong et al., 2009; Lo et al., 2010; Liao et al., 2011), it is not sufficient to solve the ''fiber crossing'' problem, owing to the native limitations of deterministic tractography algorithms. To solve the problem, a few advanced imaging technologies have been proposed, such as diffusion spectrum imaging (DSI) (Schmahmann et al., 2007; Hagmann et al., 2008) and high angular resolution diffusion imaging (HARDI), with a Q-ball reconstruction of multiple fiber orientations (Hess et al., 2006). Furthermore, the probability tractography method (Behrens et al., 2007; Iturria-Medina et al., 2010) may be helpful to overcome the ''fiber crossing'' problem. Fourth, in the current work, AAL atlas is adopted, which is based of delineation of a single brain MRI. In the future, we will try more precise automated labeling technique that allows for inter-subject variability, such as the one provided by Heckemann et al. (2006). Finally, only 18 patients with CAE were recruited in our current study. A larger sample might allow additional abnormalities of structural connectivity to be associated with CAE.

Conclusions

In the present study, we found alterations in the complex structural brain network organization of patients with CAE. These results demonstrate the disrupted topological organization of the structural network for the first time. The decreased connectivity and efficiency in the structural network may provide the anatomical evidence to explain the functional abnormalities in CAE. Moreover, decreased connectivity was identified in three sub-networks, including orbitofrontal nodes and sub-cortical nodes. These sub-networks might reflect altered structural pathways in the basal ganglia-thalamocortex, which is a core circle for the generation and propagation of SWDs in CAE. Our results suggest that the sub-network composed of the orbitofrontal cortex nodes might be a key network for the epileptic activity observed in CAE.

Disclosure of Conflicts of Interest

We confirm that we have read the Journal's position on issues involved in ethical publication and affirm that this report is consistent with those guidelines. None of the authors has any conflict of interest to disclose.

Acknowledgments

The authors are grateful to the anonymous reviewers for their comments and suggestions, which greatly improved the paper. The authors also express appreciation to Dr. Jiehui HU and Dr. Shan Gao for English language. This project was funded by grants from the 973 project 2011CB707803, the National Nature Science Foundation of China (81271547, 81160166, 81100974, 81071222, and 91232725). This study was also sponsored by Natural Science Foundation of Hainan Province of China (No. 811218).

References

Achard, S., Bullmore, E., 2007. Efficiency and cost of economical brain functional networks. PLoS Computational Biology 3, e17.

Achard, S., Salvador, R., Whitcher, B., Suckling, J., Bullmore, E., 2006. A resilient, low-frequency, small-world human brain functional network with highly connected association cortical hubs. Journal of Neuroscience 26, 63—73.

Assaf, B.A., Mohamed, F.B., Abou-Khaled, K.J., Williams, J.M., Yazeji, M.S., Haselgrove, J., Faro, S.H., 2003. Diffusion tensor imaging of the hippocampal formation in temporal lobe epilepsy. American Journal of Neuroradiology 24, 1857.

Bai, F., Shu, N., Yuan, Y., Shi, Y., Yu, H., Wu, D., Wang, J., Xia, M., He, Y., Zhang, Z., 2012. Topologically convergent and divergent structural connectivity patterns between patients with remitted geriatric depression and amnestic mild cognitive impairment. Journal of Neuroscience 32, 4307—4318.

Bai, X., Guo, J., Killory, B., Vestal, M., Berman, R., Negishi, M., Danielson, N., Novotny, E., Constable, R., Blumenfeld, H., 2011. Resting functional connectivity between the hemispheres in childhood absence epilepsy. Neurology 76, 1960.

Basser, P.J., Pajevic, S., Pierpaoli, C., Duda, J., Aldroubi, A., 2000. In vivo fiber tractography using DT-MRI data. Magnetic Resonance in Medicine 44, 625—632.

Beaulieu, C., 2002. The basis of anisotropic water diffusion in the nervous system—a technical review. NMR in Biomedicine 15, 435—455.

Behrens, T., Berg, H.J., Jbabdi, S., Rushworth, M., Woolrich, M., 2007. Probabilistic diffusion tractography with multiple fibre orientations: what can we gain? Neuroimage 34, 144—155.

Bernhardt, B.C., Chen, Z., He, Y., Evans, A.C., Bernasconi, N., 2011. Graph-theoretical analysis reveals disrupted small-world organization of cortical thickness correlation networks in temporal lobe epilepsy. Cerebral Cortex 21, 2147—2157.

Bullmore, E., Sporns, O., 2009. Complex brain networks: graph theoretical analysis of structural and functional systems. Nature Reviews Neuroscience 10, 186—198.

Caplan, R., Levitt, J., Siddarth, P., Wu, K.N., Gurbani, S., Sankar, R., Shields, W.D., 2009. Frontal and temporal volumes in childhood absence epilepsy. Epilepsia 50, 2466—2472.

Caplan, R., Siddarth, P., Stahl, L., Lanphier, E., Vona, P., Gurbani, S., Koh, S., Sankar, R., Shields, W.D., 2008. Childhood absence epilepsy: behavioral, cognitive, and linguistic comorbidities. Epilepsia 49, 1838—1846.

Carney, P.W., Masterton, R.A.J., Flanagan, D., Berkovic, S.F., Jackson, G.D., 2012. The frontal lobe in absence epilepsy EEG-fMRI findings. Neurology 78, 1157—1165.

Catani, M., Howard, R.J., Pajevic, S., Jones, D.K., 2002. Virtual in vivo interactive dissection of white matter fasciculi in the human brain. Neuroimage 17, 77—94.

Chahboune, H., Mishra, A.M., DeSalvo, M.N., Staib, L.H., Purcaro, M., Scheinost, D., Papademetris, X., Fyson, S.J., Lorincz, M.L., 2009. DTI abnormalities in anterior corpus callosum of rats with spike-wave epilepsy. Neuroimage 47, 459—466.

Chen, Q., Lui, S., Li, C.X., Jiang, L.J., Ou-Yang, L., Tang, H.H., Shang, H.F., Huang, X.Q., Gong, Q.Y., Zhou, D., 2008. MRI-negative refractory partial epilepsy: role for diffusion tensor imaging in high field MRI. Epilepsy Research 80, 83—89.

Ciccarelli, O., Catani, M., Johansen-Berg, H., Clark, C., Thompson, A., 2008. Diffusion-based tractography in neurological disorders: concepts, applications, and future developments. Lancet Neurology 7, 715—727.

Concha, L., Livy, D.J., Beaulieu, C., Wheatley, B.M., Gross, D.W., 2010. In vivo diffusion tensor imaging and histopathology of the fimbria-fornix in temporal lobe epilepsy. Journal of Neuroscience 30, 996—1002.

Crunelli, V., Leresche, N., 2002. Childhood absence epilepsy: genes, channels, neurons and networks. Nature Reviews Neuroscience 3, 371—382.

Ellison-Wright, I., Bullmore, E., 2009. Meta-analysis of diffusion tensor imaging studies in schizophrenia. Schizophrenia Research 108, 3—10.

Engel Jr., J., 2001. A proposed diagnostic scheme for people with epileptic seizures and with epilepsy: report of the ILAE Task Force on Classification and Terminology. Epilepsia 42, 796—803.

Eriksson, S.H., Rugg-Gunn, F.J., Symms, M.R., Barker, G.J., Duncan, J.S., 2001. Diffusion tensor imaging in patients with epilepsy and malformations of cortical development. Brain 124, 617.

Glauser, T.A., Cnaan, A., Shinnar, S., Hirtz, D.G., Dlugos, D., Masur, D., Clark, P.O., Capparelli, E.V., Adamson, P.C., 2010. Ethosuximide, valproic acid, and lamotrigine in childhood absence epilepsy. New England Journal of Medicine 362, 790—799.

Gong, G., He, Y., Concha, L., Lebel, C., Gross, D.W., Evans, A.C., Beaulieu, C., 2009. Mapping anatomical connectivity patterns of human cerebral cortex using in vivo diffusion tensor imaging tractography. Cerebral Cortex 19, 524—536.

Gotman, J., Grova, C., Bagshaw, A., Kobayashi, E., Aghakhani, Y., Dubeau, F., 2005. Generalized epileptic discharges show thalamocortical activation and suspension of the default state of the brain. Proceedings of the National Academy of Sciences of the United States of America 102, 15236—15240.

Gupta, D., Ossenblok, P., Van Luijtelaar, G., 2011. Space—time network connectivity and cortical activations preceding spike wave discharges in human absence epilepsy: a MEG study. Medical and Biological Engineering and Computing, 1—11.

Hagmann, P., Cammoun, L., Gigandet, X., Meuli, R., Honey, C.J., Wedeen, V.J., Sporns, O., 2008. Mapping the structural core of human cerebral cortex. PLoS Biology 6, 1479—1493.

Heckemann, R.A., Hajnal, J.V., Aljabar, P., Rueckert, D., Hammers, A., 2006. Automatic anatomical brain MRI segmentation combining label propagation and decision fusion. Neuroimage 33, 115—126.

Henkin, Y., Sadeh, M., Kivity, S., Shabtai, E., Kishon-Rabin, L., Gadoth, N., 2005. Cognitive function in idiopathic generalized epilepsy of childhood. Developmental Medicine & Child Neurology 47, 126—132.

Hess, C.P., Mukherjee, P., Han, E.T., Xu, D., Vigneron, D.B., 2006. Q-ball reconstruction of multimodal fiber orientations using the spherical harmonic basis. Magnetic Resonance in Medicine 56, 104—117.

Honey, C.J., Kotter, R., Breakspear, M., Sporns, O., 2007. Network structure of cerebral cortex shapes functional connectivity on multiple time scales. Proceedings of the National Academy of Sciences of the United States of America 104, 10240—10245.

Honey, C.J., Sporns, O., Cammoun, L., Gigandet, X., Thiran, J.P., Meuli, R., Hagmann, P., 2009. Predicting human resting-state functional connectivity from structural connectivity. Proceedings of the National Academy of Sciences of the United States of America 106, 2035—2040.

Iturria-Medina, Y., Fernández, A.P., Hernández, P.V., Pentón, L.G., Canales-Rodríguez, E.J., Melie-Garcia, L., Castellanos, A.L., Ortega, M.O., 2011. Automated discrimination of brain pathological state attending to complex structural brain network properties: the shiverer mutant mouse case. PLoS ONE 6, e19071.

Iturria-Medina, Y., Perez Fernandez, A., Morris, D.M., Canales-Rodriguez, E.J., Haroon, H.A., Garcia Penton, L., Augath, M., Galan Garcia, L., Logothetis, N., Parker, G.J.M., Melie-Garcia, L., 2010. Brain hemispheric structural efficiency and interconnectivity rightward asymmetry in human and nonhuman primates. Cerebral Cortex 21, 56—67.

Iturria-Medina, Y., Sotero, R.C., Canales-Rodríguez, E.J., Alemán-Gómez, Y., Melie-García, L., 2008. Studying the human brain anatomical network via diffusion-weighted MRI and Graph Theory. Neuroimage 40, 1064—1076.

Jones, D.K., 2004. The effect of gradient sampling schemes on measures derived from diffusion tensor MRI: a Monte Carlo study†. Magnetic Resonance in Medicine 51, 807—815.

Kim, H., Harrison, A., Kankirawatana, P., Rozzelle, C., Blount, J., Torgerson, C., Knowlton, R., 2013. Major white matter fiber changes in medically intractable neocortical epilepsy in children: a diffusion tensor imaging study. Epilepsy Research 103, 211—220.

Kwan, P., Brodie, M.J., 2001. Neuropsychological effects of epilepsy and antiepileptic drugs. Lancet-London, 216—222.

Latora, V., Marchiori, M., 2001. Efficient behavior of small-world networks. Physical Review Letters 87, 198701.

Li, Q., Luo, C., Yang, T., Yao, Z., He, L., Liu, L., Xu, H., Gong, Q., Yao, D., Zhou, D., 2009. EEG-fMRI study on the interictal and ictal generalized spike-wave discharges in patients with childhood absence epilepsy. Epilepsy Research 87, 160—168.

Liao, W., Zhang, Z., Pan, Z., Mantini, D., Ding, J., Duan, X., Luo, C., Lu, G., Chen, H., 2010. Altered functional connectivity and small-world in mesial temporal lobe epilepsy. PLoS ONE 5, e8525.

Liao, W., Zhang, Z., Pan, Z., Mantini, D., Ding, J., Duan, X., Luo, C., Wang, Z., Tan, Q., Lu, G., 2011. Default mode network abnormalities in mesial temporal lobe epilepsy: a study combining fMRI and DTI. Human Brain Mapping 32, 883—895.

Liu, M., Concha, L., Beaulieu, C., Gross, D.W., 2011. Distinct white matter abnormalities in different idiopathic generalized epilepsy syndromes. Epilepsia 52, 2267—2275.

Lo, C.Y., Wang, P.N., Chou, K.H., Wang, J., He, Y., Lin, C.P., 2010. Diffusion tensor tractography reveals abnormal topological organization in structural cortical networks in Alzheimer's disease. Journal of Neuroscience 30, 16876—16885.

Luo, C., Li, Q., Lai, Y., Xia, Y., Qin, Y., Liao, W., Li, S., Zhou, D., Yao, D., Gong, Q., 2011a. Altered functional connectivity in default mode network in absence epilepsy: a resting-state fMRI study. Human Brain Mapping 32, 438—449.

Luo, C., Li, Q., Xia, Y., Lei, X., Xue, K., Yao, Z., Lai, Y., Liao, W., Zhou, D., Valdes-Sosa, P.A., 2012. Resting state basal ganglia network in idiopathic generalized epilepsy. Human Brain Mapping 33, 1279—1294.

Luo, C., Xia, Y., Li, Q., Xue, K., Lai, Y., Gong, Q., Zhou, D., Yao, D., 2011b. Diffusion and volumetry abnormalities in subcortical nuclei of patients with absence seizures. Epilepsia 52, 1092—1099.

Mori, S., Crain, B.J., Chacko, V., Van Zijl, P., 1999. Three dimensional tracking of axonal projections in the brain by magnetic resonance imaging. Annals of Neurology 45, 265—269.

Newman, M.E.J., 2003. The structure and function of complex networks. SIAM Review, 167—256.

O'Muircheartaigh, J., Vollmar, C., Barker, G.J., Kumari, V., Symms, M.R., Thompson, P., Duncan, J.S., Koepp, M.J., Richardson, M.P., 2012. Abnormal thalamocortical structural and functional connectivity in juvenile myoclonic epilepsy. Brain 135, 3635—3644.

Onnela, J.P., Saramäki, J., Kertész, J., Kaski, K., 2005. Intensity and coherence of motifs in weighted complex networks. Physical Review E 71, 065103.

Ortinski, P., Meador, K.J., 2004. Cognitive side effects of antiepileptic drugs. Epilepsy & Behavior 5, 60—65.

Pavone, P., Bianchini, R., Trifiletti, R., Incorpora, G., Pavone, A., Parano, E., 2001. Neuropsychological assessment in children with absence epilepsy. Neurology 56, 1047—1051.

Pierpaoli, C., Basser, P.J., 1996. Toward a quantitative assessment of diffusion anisotropy. Magnetic Resonance in Medicine 36, 893—906.

Ponten, S., Bartolomei, F., Stam, C., 2007. Small-world networks and epilepsy: graph theoretical analysis of intracerebrally recorded mesial temporal lobe seizures. Clinical Neurophysiology 118, 918—927.

Qi, R., Xu, Q., Zhang, L.J., Zhong, J., Zheng, G., Wu, S., Zhang, Z., Liao, W., Zhong, Y., Ni, L., 2012. Structural and functional abnormalities of default mode network in minimal hepatic encephalopathy: a study combining DTI and fMRI. PLoS ONE 7, 1—9.

Raichle, M.E., MacLeod, A.M., Snyder, A.Z., Powers, W.J., Gusnard, D.A., Shulman, G.L., 2001. A default mode of brain function. Proceedings of the National Academy of Sciences of the United States of America 98, 676—682.

Rubinov, M., Sporns, O., 2010. Complex network measures of brain connectivity: uses and interpretations. Neuroimage 52, 1059—1069.

Rugg-Gunn, F.J., Eriksson, S.H., Symms, M.R., Barker, G.J., Duncan, J.S., 2001. Diffusion tensor imaging of cryptogenic and acquired partial epilepsies. Brain 124, 627.

Schmahmann, J.D., Pandya, D.N., Wang, R., Dai, G., D'Arceuil, H.E., de Crespigny, A.J., Wedeen, V.J., 2007. Association fibre pathways of the brain: parallel observations from diffusion spectrum imaging and autoradiography. Brain 130, 630—653.

Shehata, G.A., Bateh, A.E.M., 2009. Cognitive function, mood, behavioral aspects, and personality traits of adult males with idiopathic epilepsy. Epilepsy & Behavior 14, 121—124.

Shu, N., Liu, Y., Li, K.C., Duan, Y.Y., Wang, J., Yu, C.S., Dong, H.Q., Ye, J., He, Y., 2011. Diffusion tensor tractography reveals disrupted topological efficiency in white matter structural networks in multiple sclerosis. Cerebral Cortex 21, 2565—2577.

Sporns, O., Chialvo, D., Kaiser, M., Hilgetag, C., 2004. Organization, development and function of complex brain networks. Trends in Cognitive Sciences 8, 418—425.

Tenney, J.R., Glauser, T.A., 2013. The current state of absence epilepsy: can we have your attention? Epilepsy Currents 13, 135—140.

Tucker, D.M., Brown, M., Luu, P., Holmes, M.D., 2007. Discharges in ventromedial frontal cortex during absence spells. Epilepsy & Behavior 11, 546—557.

Tzourio-Mazoyer, N., Landeau, B., Papathanassiou, D., Crivello, F., Etard, O., Delcroix, N., Mazoyer, B., Joliot, M., 2002. Automated anatomical labeling of activations in SPM using a macroscopic anatomical parcellation of the MNI MRI single-subject brain. Neuroimage 15, 273—289.

Vaessen, M.J., Jansen, J.F.A., Vlooswijk, M.C.G., Hofman, P.A.M., Majoie, H.J.M., Aldenkamp, A.P., Backes, W.H., 2012. White matter network abnormalities are associated with cognitive decline in chronic epilepsy. Cerebral Cortex (New York, NY: 1991) 22, 2139—2147.

Vollmar, C., O'Muircheartaigh, J., Symms, M., Barker, G., Thompson, P., Kumari, V., Stretton, J., Duncan, J., Richardson, M., Koepp, M., 2012. Altered microstructural connectivity in juvenile myoclonic epilepsy: the missing link. Neurology 78, 1555—1559.

Wakana, S., Jiang, H., Nagae-Poetscher, L.M., Van Zijl, P., Mori, S., 2004. Fiber tract-based atlas of human white matter anatomy. Radiology 230, 77—87.

Wang, B., Fan, Y., Lu, M., Li, S., Song, Z., Peng, X., Zhang, R., Lin, Q., He, Y., Wang, J., 2013. Brain anatomical networks in world class gymnasts: a DTI tractography study. Neuroimage 65, 476—487.

Wang, R., Benner, T., Sorensen, A., Wedeen, V., 2007. Diffusion toolkit: a software package for diffusion imaging data processing and tractography. International Society for Magnetic Resonance in Medicine 15.

Watts, D.J., Strogatz, S.H., 1998. Collective dynamics of 'small-world' networks. Nature 393, 440—442.

Yang, T., Guo, Z., Luo, C., Li, Q., Yan, B., Liu, L., Gong, Q., Yao, D., Zhou, D., 2012. White matter impairment in the basal ganglia-thalamocortical circuit of drug-naive childhood absence epilepsy. Epilepsy Research 99, 267—273.

Zalesky, A., Cocchi, L., Fornito, A., Murray, M.M., Bullmore, E., 2012. Connectivity differences in brain networks. Neuroimage 60, 1055—1062.

Zalesky, A., Fornito, A., Bullmore, E.T., 2010. Network-based statistic: identifying differences in brain networks. Neuroimage 53, 1197—1207.

Zhang, J., Wang, J., Wu, Q., Kuang, W., Huang, X., He, Y., Gong, Q., 2011a. Disrupted brain connectivity networks in drug-naive, first-episode major depressive disorder. Biological Psychiatry 70, 334—342.

Zhang, Z., Liao, W., Chen, H., Mantini, D., Ding, J.R., Xu, Q., Wang, Z., Yuan, C., Chen, G., Jiao, Q., 2011b. Altered functional—structural coupling of large-scale brain networks in idiopathic generalized epilepsy. Brain 134, 2912—2928.